Integrated Air and Space Traffic Management: An Agent-Based Simulation for Analysis of Space-Launch Impact on Air Traffic

Zhengyi Wang, Imen Dhief, Wei Zhou, Sameer Alam
Air Traffic Management Research Institute
Nanyang Technological University
Singapore, Singapore
{zhengyi.wang, imen.dhief, wei.zhou, sameeralam}@ntu.edu.sg

Henk A. P. Blom
Faculty of Aerospace Engineering
Delft University of Technology
Delft, The Netherlands
h.a.p.blom@tudelft.nl

Sven Kaltenhäuser, Tobias Rabus
Institute of Flight Guidance
German Aerospace Center (DLR)
Braunschweig, Germany
{sven.Kaltenhaeuser, tobias.rabus}@dlr.de

***Abstract*—The recent surge in space launch activities, driven by the emergence of commercial space launches, has compelled the aviation and space launch sectors to collaborate for the safe and efficient integration of space launch activities. This paper introduces an agent-based modeling (ABM) and simulation framework designed to assess the impact of spacecraft launches on air traffic within an integrated air and space traffic management system. The proposed framework incorporates various agents involved in the execution phase of space launches and considers the interactions and coordination between air traffic management and space traffic management. The paper firstly provides a comprehensive overview of the current state of space launch operations and their effects. Then, a general agent-based model is developed for space launch execution phase in order to gain an understanding of various entities involved in a space launch activity as well as the interactions among these entities. Using Monte-Carlo simulations based on the ABM, the paper assesses the impact on air traffic operations in the event of a space launch failure. In each simulation, various factors are taken into account, including launch site position, launch slot, failure probability during the execution phase, debris dispersion, and time delay in Air Traffic Management (ATM)/Space Traffic Management (STM) coordination. To demonstrate the practical application of the proposed framework in an operational context, the paper presents a case study of a sea-based space launch in the Singapore FIR. The paper makes a valuable contribution to the field of air and space traffic management by addressing the need for innovative strategies to ensure the safe sharing ofairspace among different stakeholders.**

***Keywords*—Space traffic management, Air traffic management, Airspace integration, Impact assessment, Agent-based modeling, Monte-Carlo simulation, Debris hazard area**

1. Introduction

Currently, airspace accommodates a diverse range of users, including aircraft, drones, and space shuttles [1]. Traditionally, the management of airspace utilization involved segregating different operations, a method that proved effective when airspace was primarily allocated for air traffic, and other users were infrequent. However, as both air traffic and space activities have grown substantially, there is an urgent necessity to develop innovative and adaptable strategies to ensure the safe and efficient sharing of airspace among these varied stakeholders.

Space has transformed into a crucial commercial domain, seeing the active involvement of multiple nations and private corporations in space endeavors such as SpaceX, Virgin Galactic, United Launch Alliance, Arianespace, and Blue Origin. Indeed, space-based assets have progressively become integral to our daily existence, as various industries and sectors depend heavily on satellite communications, remote sensing, and global navigation satellite system (GNSS) technology. Currently, there are 35 spaceports and launch facilities worldwide possess the capability to launch satellites or spacecraft into sub-orbit, orbit, and beyond [2]. Driven by technological advancements and the expansion of space operators in recent years, there has been an exponential increase in space launch activities globally [3].

This phenomenon has emphasized the urgency of exploring innovative procedures and approaches in Space Traffic Management (STM) and their seamless integration with global Air Traffic Management (ATM) system, especially in the near future. Representative related ATM/STM initiatives are proposed by SESAR Joint Undertaking [4, 5], DLR [6], NASA [7], and FAA [8]. A common thread among these projects is the prioritization of safety in ATM/STM integration.

The overarching objective is to examine potential impacts, risks, vulnerabilities, and hazards in transportation systems through suitable analytical tools [9]. In traditional STM, extensive research has focused on hazards directly related to spacecraft systems during the pre-mission and execution phases of space launches [10–19], which are summarized in Table I. However, if a spacecraft accident occurs, the direct

SESAR Innovation Days
27-30 November 2023
Seville

impact to commercial air traffic remains unclear. Instead, [15, 16, 20] assessed the debris impact of space launch failures on commercial air traffic within the ATM/STM framework. These studies employed equations of motion to model spacecraft trajectory and debris dispersion, then assessing the debris hazard to impacted airspace. The analysis models include system-based models [11, 13] and probabilistic models [10, 18, 19]. They can be regarded as pioneering studies that contribute to ATM/STM integration, as they have undertaken the initial assessment of space launch hazard on ATM. Nevertheless, most of these studies primarily focused on assessing the potential debris hazards to impacted airspace, rather than investigating their direct impact on air traffic by considering actual flight plans and aircraft trajectories. Furthermore, there has been limited research that considered interaction between STM and ATM, especially in the context of risk mitigation processes involving STM and ATM systems and entities if space launch failures occur.

The objective of this study is to introduce a framework to evaluate the comprehensive impact of space launch hazards on air traffic, taking into consideration the real air traffic situation and the coordination between ATM and STM. As space launch is an open multi-complex socio-technical system, these characteristics cannot be well captured by event-based modeling widely used in the aforementioned literature. Agent-based modeling (ABM) has been proven to be effective in analyzing complex socio-technical systems [21]. ABM aims to understand the behaviour of the system by modeling the actions and interactions between the involving agents. To the author's knowledge, this study represents one of the pioneering applications of ABM in the analysis of space launch hazard. The contributions of this paper are:

- The development of an ABM model for space launch execution phase in order to gain a comprehensive understanding of various entities involved in a space launch activity as well as the interactions among these entities during the execution phase.
- The implementation of a Monte-Carlo simulation based on the ABM for analysis of air traffic operations in the event of space launch failure. In each simulation, various random factors are taken into account, including launch site position, launch slot, failure probability during the execution phase, debris dispersion, and time delay in ATM/STM coordination.
- A comprehensive analysis of the potential impact defined as various performance metrics of debris hazard areas, and the required rerouting of aircraft for a sea-based launch.

The concept diagram of the proposed agent-based framework for air and space traffic management is highlighted in Figure 1. In case of a spacecraft failure, the mission control center calculates the debris area and shares this information with Air Navigation Service Providers (ANSPs), who then relay it to Air Traffic Controllers (ATC) via Notice to Airmen (NOTAM). Consequently, the ATC reroute the flights in order to avoid the calculated debris area.

2. Context and Background of Space Launch

A. Overview of space launch operations

The space launch process can be generally classified into three primary phases: pre-mission, execution, and post-mission [22].A detailed description of the process and its associated phases is depicted in Figure 2.

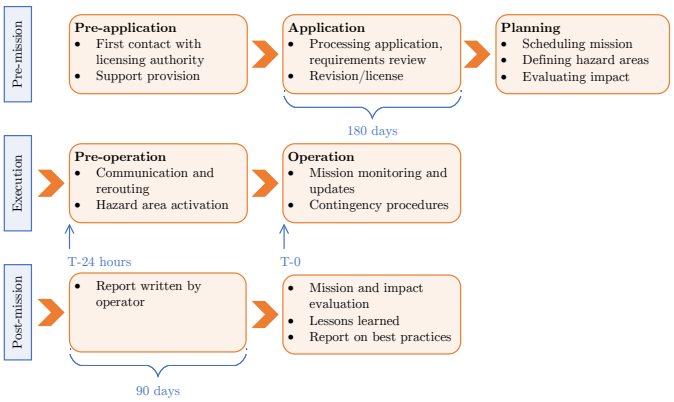

Figure 2: Phases and associated procedures for typical space launch operations

During the pre-mission phase, any launch activity commences with the pre-application process, which is typically initiated months or even years prior to the actual operation. This process serves as the initial step for the operator to establish contact with the responsible regulator. Once it is sufficiently complete, the actual application process should commence promptly, which generally last for 180 days. Subsequently, in the planning process, risk areas in terms of air traffic and maritime should be defined and then be communicated.

The execution phase of the launch process can be further divided into pre-operation and the operational phase. The pre-operation phase begins at T-24 hours. Key stakeholders are informed and alternate routes are established, while hazardous areas are identified. The operation phase begins at T-0, in which the mission is continuously monitored and updated, with pre-planned contingency procedures in place to address any unexpected issues. During the execution phase, the potential hazards associated with space launches have the most significant impact on air traffic, and interactions between the agents are most intensive. The primary focus of the current work lies in the execution phase, with the objective of assessing the risks prevalent in this phase.

To conclude the mission, it is necessary for the spacecraft operator to submit a report to the appropriate regulatory authority within a specified timeframe after the operation, e.g. 90 days. This report serves as a valuable document for subsequent investigations by the regulatory authority. Moreover, a comprehensive analysis of the potential impacts of the space operation on the air traffic system should be conducted. It is also important to extract and derive best practices and lessons learned from the mission.

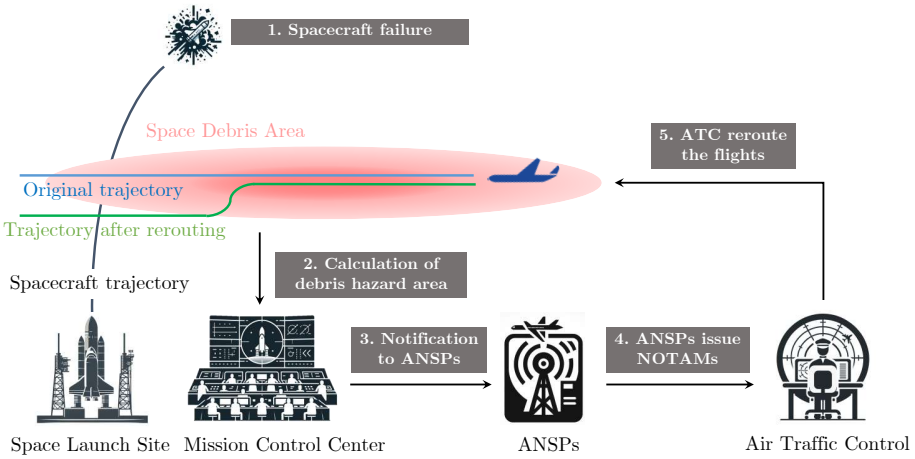

Figure 1: Concept diagram of the proposed agent-based and simulation framework for air and space traffic management in the event of space vehicle failure and resulting debris hazard to air traffic.

TABLE I: Summary of state-of-the-art space launch impact assessment studies

Reference	Flight phases	Specific stage or process	Launch type	Model
[10]	Pre-mission	technical zone, launch zone, and ground measure-control system	ground-based	fuzzy Bayesian network
[11]	Pre-mission	space launch vehicle development	ground-based	Systems engineering capability model
[12]	Execution	debris fields and gas clouds	ground-based	debris sheltering model
[13]	Pre-mission and Execution	preparation and implementation	ground-based	gray relational analysis
[14]	Execution	ascent	ground-based	dynamic scenario-based simulation model
[15]	Execution	debris during the flight and from failures	ground-based	Monte Carlo simulation
[16]	Execution	debris during the flight and from failures	ground-based	Monte Carlo simulation
[17]	Execution	debris, blast and toxic hazard	ground-based	Monte Carlo simulation
[18]	Execution	collision	ground-based	Bayesian inference
[19]	Execution	main propulsion systems and shuttle subsystems	ground-based	probabilistic risk analysis
Our study	Execution	impact to air traffic	sea-based	agent-based model

B. General process of on-trajectory space vehicle failure

In case of a catastrophic failure of space launch, debris could fall down through a range of airspace. Without intervention, Aircraft (A/C) could be exposed to falling debris within minutes. The duration of debris falling can range from 20 to 40 minutes, depending on the failure altitude [23]. In such instances, Air Traffic Controllers (ATCos) are responsible of diverting flights away from the debris area and offer alternative rerouting options. Throughout the duration of debris, Aircraft are strongly advised to avoid traversing this area at any altitude.

The risk of space launch failure to air traffic is quantified as the probability of impact with debris that is able to cause a casualty for A/C during a launch or reentry operation. According to the Code of Federal Regulations (14 CFR) [24], this probability must be below the threshold of 10^{-6} per launch [18].

To protect the commercial A/C from the potential hazard associated with space launch failure in the execution phase, close collaboration with the affected Air Navigation Service Providers (ANSPs) is essential as they are responsible to review and issue the NOTAMs to their Flight Information Regions (FIRs). In the case of non-nominal events, debris hazard area will be computed using sophisticated modeling techniques in the mission control center, acting as an accurate estimation of the debris area. The coordinates of the hazard area are subsequently transmitted to Air Traffic Control (ATC) in a digital format. Implementing this approach necessitates the utilization of advanced, automated, and interconnected systems.

3. Agent-Based Modelling of Execution Phase in Space Launch

A. Agent-based modelling

Agent-Based Modeling (ABM) has proven its effectiveness in analyzing complex socio-technical systems [21]. In this approach, agents interact within a simulated airspace environment, allowing for the dynamic exploration of various scenarios. ABM is able to analyze potential disruptions to air traffic caused by space launches, taking into account factors such as launch timing, trajectory, and airspace restrictions.

Therefore, we develop an agent-based model to gain a comprehensive understanding of the complex interactions among entities involved in the execution phase. The agents involved in the coordination between space launch operations and air traffic are listed as follows:

1) ANSP: ANSP_i, $i = 1, \cdots, N_\text{A}$, where N_A is the number of ANSPs.

2) ATC system: ATCS_i, $i = 1, \cdots, N_\mathrm{A}$.
3) ATCO: $\mathrm{ATCO}_{i,j}$, $i = 1, \cdots, N_\mathrm{A}$, $j = 1, \cdots, N^i_\mathrm{T}$, where N^i_T is the number of ATCos in i-th ANSP.
4) A/C: $\mathrm{AC}_{i,j}$, $i = 1, \cdots, N_\mathrm{A}$, $j = 1, \cdots, N^i_\mathrm{AC}$, where N^i_AC is the number of A/C controlled by the i-th ANSP.
5) A/C pilot: $\mathrm{ACP}_{i,j,k}$, $i = 1, \cdots, N_\mathrm{A}$, $j = 1, \cdots, N^i_\mathrm{AC}$, k is used to distinguish between pilot flying (PF) and pilot not flying (PNF), and $k = 1, 2$.
6) Communication system: CS_n, $n = 1, \cdots, N_\mathrm{CS}$, where N_CS is the number of communication systems depending on the service type.
7) Surveillance system: SS_i, $i = 1, \cdots, N_\mathrm{SS}$, where N_SS is the number of surveillance system depending on the service type.
8) Navigation system: NS_i, $i = 1, \cdots, N_\mathrm{NS}$, where N_NS is the number of navigation system depending on the service type.
9) Mission control center: MCC.
10) Mission control system: MCS.
11) Mission controller: MC_i, $i = 1, \cdots, N_\mathrm{M}$, where N_M is the number of mission controllers in the mission control center.
12) Space vehicle: SV.
13) Space vehicle crew: SVC_i, $i = 1, \cdots, N_\mathrm{SVC}$, where N_SVC is the number of space vehicle crew.
14) Meteorological service: MS.
15) Local emergency service: LES_i, $i = 1, \cdots, N_\mathrm{L}$, where N_L is the number of local emergency services.
16) Maritime control center: MaCC_i, $i = 1, \cdots, N_M$, where N_M is the number of maritime control centers.
17) Ship: $\mathrm{S}_{i,j}$, $i = 1, \cdots, N_\mathrm{M}$, $j = 1, \cdots, N^i_\mathrm{S}$, where N^i_T is the number of ships controlled by i-th maritime control center.
18) Ship crew: $\mathrm{SC}_{i,j,k}$, $i = 1, \cdots, N_\mathrm{M}$, $j = 1, \cdots, N^i_\mathrm{S}$, $k = 1, ..., N^{i,j}_\mathrm{SC}$, where $N^{i,j}_\mathrm{SC}$ is the number of crews of $\mathrm{S}_{i,j}$.

Among these agents, we can split them into five categories: space launch, public service, air traffic, Communication, Navigation and Surveillance (CNS), and maritime. 1)-5) relate to air traffic, 6)-8) correspond to Communication, Navigation, and Surveillance (CNS), 9)-12) relate to space launch, 13)-14) associate with public service, and 15)-17) relate to maritime. Note that maritime agents are not considered in this study due to the specific focus on air traffic impact.

The interactions between these identified agents are presented in Figure 3. The subscript i, j, k, n indicate different instances or versions of the associated agent. The arrows, including single-headed and double-headed arrows, represent the interactions and communications between agents. A bidirectional arrow signifies that the interaction or influence goes both ways. Agents belonging to the same category are grouped together in the figure.

B. Detailed description on related to air traffic

In general space launch operations, there are dynamic interactions between multiple agents at distributed units under the influence of external factors, e.g. environment.

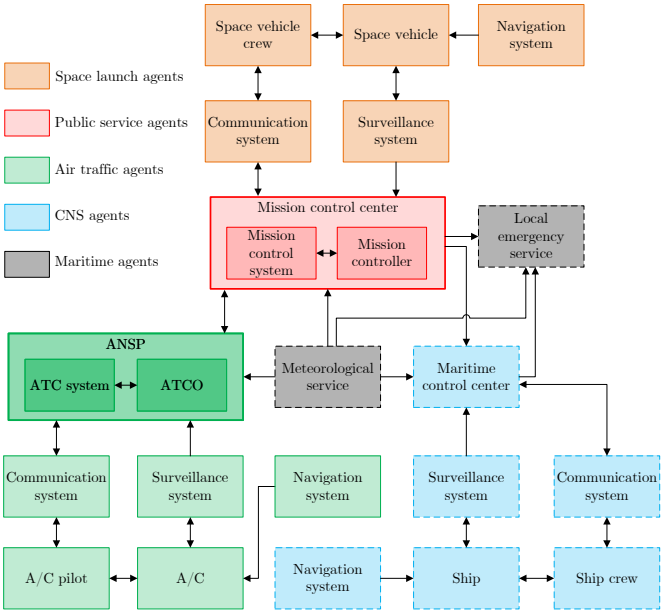

Figure 3: A schematic representation of interactions between the agents in the execution phase. The legend specifies each agent type, and agents outlined with dashed lines are not the focus of this study.

To gain a deeper understanding of the associated agent-based model, we further elaborate on the high-level agents related to air traffic and directly involved in space launch activities, including A/C and ANSPs. The entities are further categorized into four types, including proactive agents, reactive agents, high-level agents and non-agent entities. A proactive agent is capable of independently initiating actions and exhibiting adaptive behaviors, while a reactive agent can only perceive its environment and react promptly to changes that occur within it, which represents behaviors regarding stimulus-response and delayed-response. The high-level agents represent a system or entity that composed of multiple lower-level agents. A non-agent entity can be impacted by its environment, but lacks the ability to perceive it. We use different shape to represent these entity types, as shown in Figure 4.

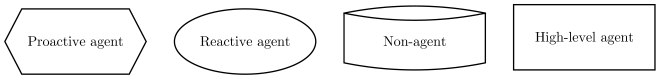

Figure 4: Legends of different types of entity. Hexagon - Proactive agent, Ellipse - Reactive agent, Cylinder - Non-agent, and Rectangle - High-level agent.

Figure 5 presents an overview of the agents of an A/C. The non-agents include weather, airspace structure, and space structure, as they cannot perceive the environment. These non-agents are considered as the inputs to the high-level agents. Weather organization belongs to proactive agent, which provide weather information to the high-level agents. The A/C is a reactive agent.

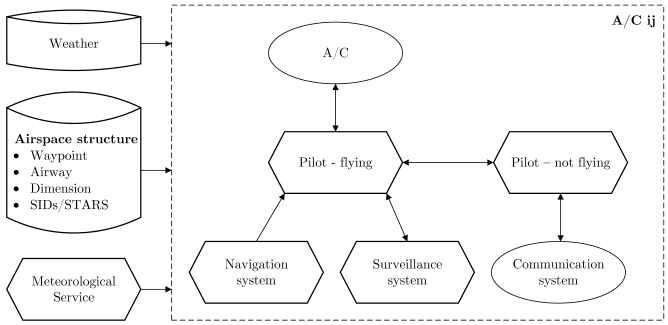

Figure 5: High-level agent overview of A/C involved in the execution phase of space launch.

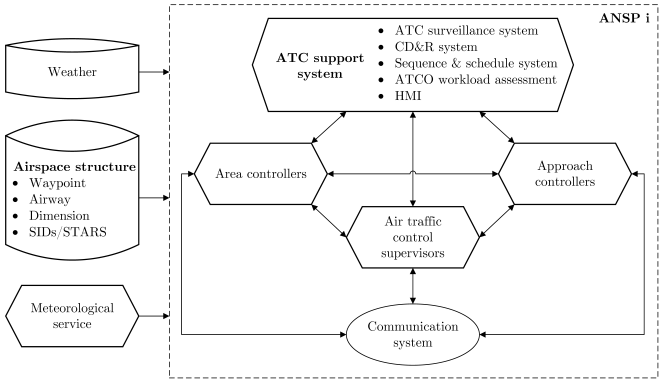

Figure 6: High-level agent overview of ANSP involved in the execution phase of space launch.

C. Description of coordination between ATM/STM in the case of space launch failure

We consider a failure scenario in the execution phase of a space launch operation. As this problem involves multiple variables that interact in complex ways, we adopt Monte-Carlo simulation to evaluate the spacecraft failure hazard to air traffic. By generating numerous random scenarios that consider factors such as launch timing, trajectory, and airspace regulations, Monte Carlo simulations provide a detailed and probabilistic view of how space launch activities affect air traffic operations, and identification of potential bottlenecks and disruptions. The procedure in each simulation is formulated as follows:

1) Arbitrarily select the position of launch site in the potential launch area and the launch slot, then compute the spacecraft trajectory based on dynamics of the spacecraft motion.
2) the occurrence time of spacecraft failure is governed by a probability distribution $p_{\mathrm{f}}(t)$ as a function of time t.
3) Information transfer about spacecraft failure to impacted air traffic for rerouting purposes:
   a) On-trajectory space vehicle failure occurs.
   b) In MCC, some MC_1 declare failure and collect state vector of SV via SSV.
   c) These MC_1 send state vector to other MC_2 related to debris hazard area computation via internal hotline.
   d) MC_2 read back, transcribe and type state vector into MCS to compute debris hazard areas.
   e) MC_2 transcribe and type out debris hazard area coordinates into traffic display of MCS.
   f) MC_2 send calculated debris hazard areas to ATCOs via data link.
   g) In each ANSP_i, the associated $\mathrm{ATCO}_{i,j}$ passes coordinates of calculated debris hazard areas to ATCS_i for display.
   h) Each $\mathrm{ATCO}_{i,j}$ assesses the air traffic situation, instructs each responsible $\mathrm{ACP}_{i,j_1,2}$ within debris hazard area to deviate from debris hazard areas, and provides the responsible $\mathrm{ACP}_{i,j_2,2}$ that approaches to debris hazard areas with rerouting options to avoid the area.
   i) The associated $\mathrm{ACP}_{i,j,1}$ receives instructions and executes $\mathrm{AC}_{i,j}$ to avoid debris hazard areas.

4. Analysis for Space Launch Failure Impact to Air Traffic

Assessing the impact of space launch failures on air traffic is crucial for understanding their overall implications. To this end, we have developed a set of representative performance metrics that are relevant to this context. For each simulation run s,

- Number of impacted flights $\hat{N}_s$: This metric counts the total number of flights that are rerouted due to space launch failures. It is calculated by tracking changes in flight paths from scheduled routes to rerouting routes during the impact period when a space launch failure:

$$\hat{N}_s = \sum_{i=1}^{N_{\mathrm{AC}}} \delta(i,s) \tag{1}$$

where

$$\delta(i,s) = \begin{cases} 1, & \text{if } f_i \in \hat{\mathscr{F}}_s \\ 0, & \text{otherwise} \end{cases} \tag{2}$$

, $\hat{\mathscr{F}}_s = \{f_i : \mathscr{R}^{i,\tau_s}_{\mathrm{sche}} \cap \mathscr{H}_s \neq \emptyset\}$ is the set of impacted flights in the simulation run s, $\mathscr{R}^{i,\tau_s}_{\mathrm{sche}}$ is the scheduled route of flight i during the debris impact time τ_s, and $\mathscr{H}_s$ is the debris hazard area in the simulation run s.
- Total delay $\hat{T}_s$: This metric calculates the total time delay experienced by the flights impacted by a space launch failure. Understanding the total delay helps in quantifying the time inefficiency introduced into the air traffic system by such events. The metric is computed by summing all the individual flight delay:

$$\hat{T}_s = \sum_{f_i \in \hat{\mathscr{F}}_s} (T^i_{\mathrm{r}} - T^i_{\mathrm{sc}}) \tag{3}$$

where T^i_{r} represents the actual flight time of f_i rerouted due to the space launch failure, and T^i_{sc} represents the scheduled flight time of f_i.

- Total extra flight distance $\hat{D}_s$: This metric calculates the total additional distance that impacted flights must travel due to rerouting around or exiting hazard areas. Extra distance is positively correlated with fuel consumption and operational costs. The metric is determined by comparing the planned flight distance with the actual distance flown for all rerouted flights and then summing these differences.

$$\hat{D}_s = \sum_{f_i \in \hat{\mathcal{F}}_s} (D_{\mathrm{r}}^i - D_{\mathrm{sc}}^i) \tag{4}$$

where D_{r}^i is the actual distance flown by f_i, and D_{sc}^i denotes the planned flight distance of f_i.

5. Simulation and Experiment

A. Experiment settings

We conduct a case study of a potential sea-based space launch in Singapore FIR. Although it is currently a concept, there are several benefits, including the proximity to the equator, minimal impact on densely populated areas, and greater flexibility in both launch timing and trajectory. The possible launch site area is situated east of Singapore over South China Sea Danger Areas, as presented in Figure 7.

The selected area is surrounded by several danger areas activated by NOTAM and do not have ATS routes traversing through it. It is free of civil flights, thereby minimizing disruptions to air traffic. The air traffic data from the Singapore FIR for the month of September 2023 is used in this study.

The trajectory of a two-stage spacecraft [25] is delineated through the utilization of a mathematical model, and the simulation is conducted in the Simulink. A space launch profile is shown in Figure 8. The trajectory has been planned to mitigate aerodynamic side loads, and this is achieved by maintaining a zero angle of attack by executing gravity turn manoeuvres. The initial angular orientation is defined as 90 degrees, accompanied by the initiation of liftoff thrust at 346,961.28 N. The propulsion system operates with a mass flow rate of 134.4kg/s [26]. The spacecraft's propellant reserves amount to 47,380lb, while the dry mass is determined to be 1,360.7kg. The remaining fuel mass stands at 21,491.26kg, and the payload is set at 5,000kg. Additionally, key parameters include a reference diameter of 1.5 m, a reference drag area of 0.075, and a distance from the nose-tip to the centre of gravity measuring 7m. The atmospheric density and pressure models employed are detailed in [27].

The activation time of debris hazard area is set as 1 hour [23]. We conduct Monte-Carlo simulation for 4,800 runs, randomly selecting launch site positions in the potential area, three potential launch slots (8:00-9:00. 12:00-13:00, 20:00-21:00), failure probability during the execution phase [16], debris dispersion, and time delay in ATM/STM coordination. For each process related to information transfer about spacecraft failure to impacted air traffic in step 3) of section 3.3, their time delays are assumed to follow uniform distributions according to current STM operations [28], in which $\tau_{\mathrm{b})} \sim \mathcal{U}(1,2)$, $\tau_{\mathrm{c})-\mathrm{d})} \sim \mathcal{U}(4,6)$, $\tau_{\mathrm{e})} \sim \mathcal{U}(2,4)$, $\tau_{\mathrm{f})} \sim \mathcal{U}(3,5)$,

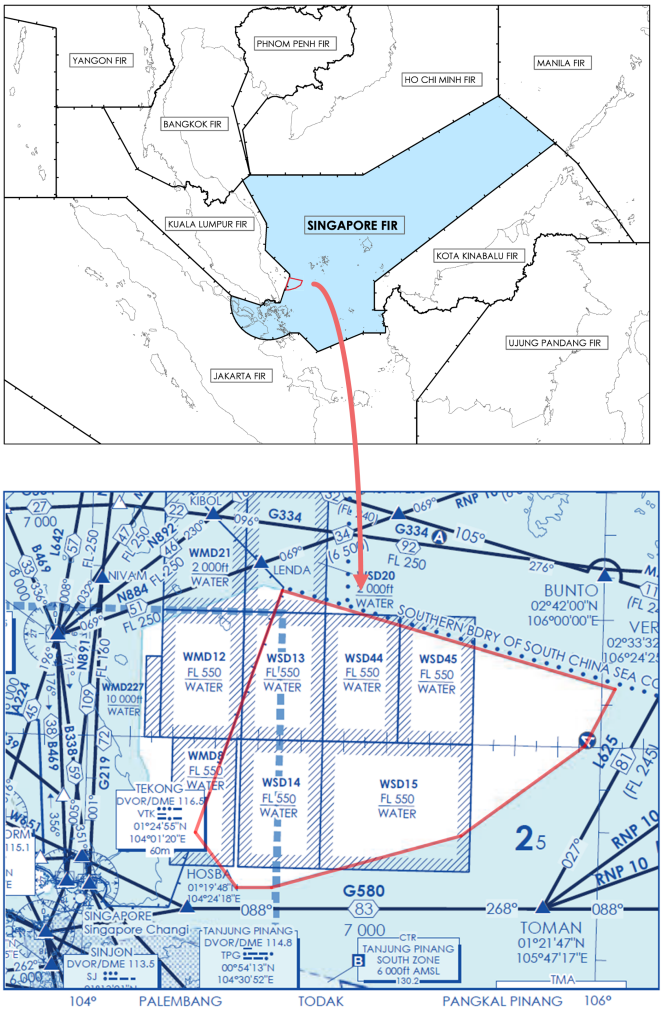

Figure 7: Potential area for sea-based space launch in Singapore FIR (red polygon).

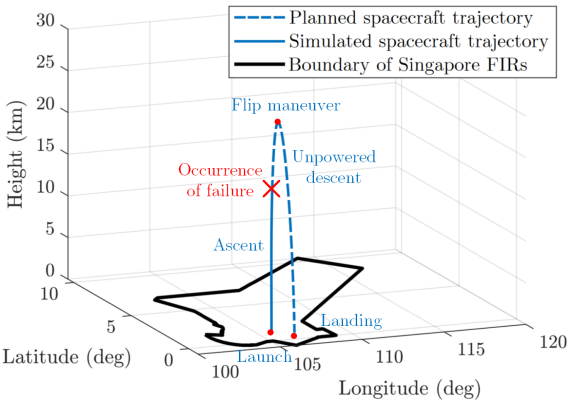

Figure 8: Visualization of a spacecraft's trajectory from launch to failure at a certain altitude in a simulation. Potentially impacted FIRs are also highlighted.

$\tau_{\mathrm{g})} \sim \mathcal{U}(2,3)$. as procedure h) depends on the air traffic density and the size of hazard area, we assume the associated time delay follows $\tau_{\mathrm{h})} \sim \mathcal{U}(3,4)$. The unit of these time delays is minutes. For simplification, the rerouting strategy for flights within the debris hazard areas is to choose the quickest

available route to exit the hazard area and then returning to the original flight plan. For aircraft that are still outside the debris hazard area when receiving the rerouting request but are scheduled to pass through the debris hazard area during its activation, the shortest path along the edge of the debris hazard area is selected as the diverted route.

B. Spacecraft trajectory and debris dispersion modeling

In the context of debris generation in case of spacecraft failures, this study uses mathematical model detailed in [20] to present the equations of motion governing the dynamics of individual debris fragments. These equations are calculated in the ECEF coordinate system, accounting for the initial conditions, external forces, and altitude evolution of each debris fragment, and tailoring the spacecraft trajectory. As shown in Figure 9, Kernel Density Estimation (KDE) [29] is applied to computed debris data to generate the debris hazard area, which is defined as the contour with a pre-defined density threshold 10^{-6} [18]. Gaussian kernel is used for density

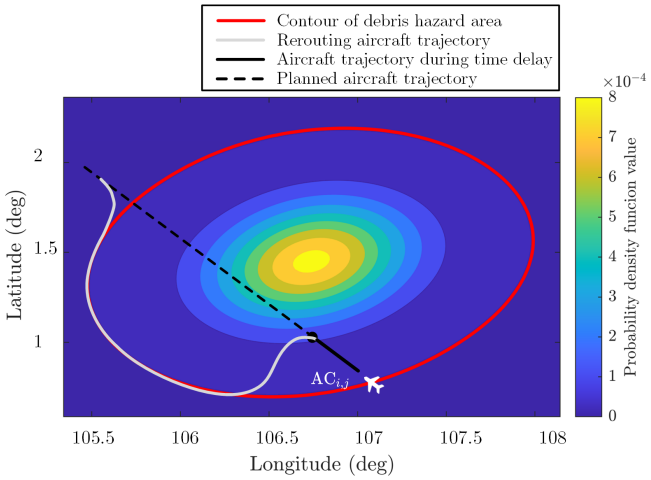

Figure 9: An illustration of rerouting aircraft within the debris hazard area generated by KDE of debris.

estimation and the bandwidth of the kernel-smoothing window is optimally selected [30]. For simplicity, the number of debris produced by spacecraft failure is assumed to follow a normal distribution $\mathcal{U}(400, 1200)$ [31].

As seen in Figure 8, the simulated spacecraft initiates its trajectory with a starting pitch angle of 90 degrees, reaches its peak altitude at 25.484 km, at the 142.67-second mark, and then undergoes a gravity turn maneuver. Subsequently, after the vertical unpowered descent, at 230.19 seconds, the spacecraft landing back to Earth's surface.

Figure 9 depicts the 2D distribution of debris from a space launch failure in a simulation run. The red contour defines the range of debris hazard area. It can be seen that more central regions indicate higher risk due to concentrated debris. An example of a impacted aircraft trajectory is showcased. After the occurrence of space launch failure, the aircraft proceed on its original course. Following a time delay in coordination between STM and ATM, the pilot was informed to exit the hazard area. The aircraft then rapidly reroutes to exit the high-risk area within the debris hazard area.

C. Experiment results

Note that, the actual route of an flight impacted by debris can be segmented into two parts: the flight route during the time delay related to ATM/STM coordination, and the rerouting flight route after the pilot receives the rerouting command. To assess the impact of the duration of time delay on air traffic, We will further assess the impact on air traffic during the time delay period and compare it to an ideal situation where no delay exists. In this ideal situation, all flights would be immediately rerouted away from the hazard area as soon as a spacecraft failure occurs. Therefore, the number of affected flights, the trajectory elongation and the total delay are computed for this scenario, and also for air traffic throughout debris impact duration. A 95% Confidence Interval (CI) for the standard normal distribution is used to present these performance metrics. The point estimate, lower and upper bounds of the results are given in Table II.

Based on the results presented in Table II, it is evident that the impact of spacecraft failure on air traffic is substantial. We might expect minimal disruptions as aircraft are immediately diverted from the hazard zone. However, the result showcases that even with instantaneous rerouting, there are still a considerable impact. Nearly 4 aircraft will enter debris hazard area under current operational time delay. In addition, a large amount of extra flight distance and delay occur in time delay stage. The longer flight routes lead to increased fuel consumption, operational costs, and subsequent environmental impacts. The total delay, indicative of the cumulative time aircraft have to spend either rerouting or due to time delay related to ATM/STM coordination, is also significant. Such prolonged delays have wider consequence on passenger schedules, airline operations, and the overall punctuality of the operation.

Even under the most ideal circumstances, the impact is noticeable. With realistic time delays, the effects will be even more significant. This demonstrates the heightened vulnerability of air traffic when faced with space launch hazards.

TABLE II: 95% CI for performance metrics in different scenarios

Metrics	95% CI		Unit
	Debris impact duration	Time delay duration	
NIF*	17.93 (17.76, 18.11)	3.67 (3.70, 3.82)	num
TEFD*	136.07 (135.51, 136.63)	37.40 (36.54, 38.26)	km
TD*	760.57 (754.13, 767.00)	263.54 (255.94, 271.14)	s

*: NIF: Number of Impacted Flights, TEFD: Total Extra Flight Distance, TD: Total Delay

To further interpret these results, box plots are utilised as a graphical tool to visualize the distribution of metrics for different launch slot. Note that the whiskers contains 90% of the data, and the box contains 50% of the data. Analyzing each performance metric from the graph, it is apparent that the air traffic experiences the least impact when the launch

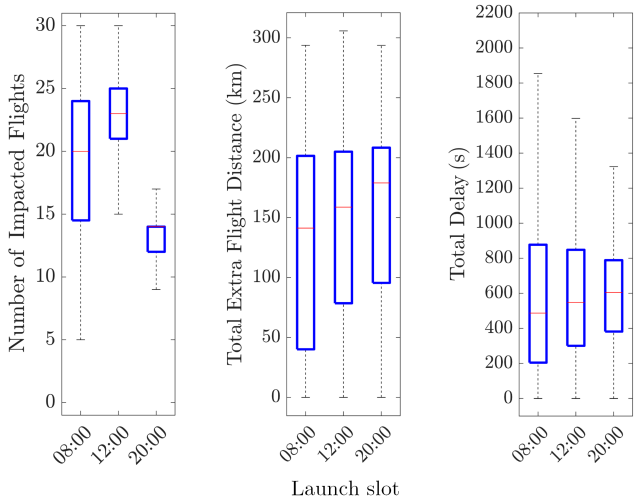

(a) Number of impacted flights (b) Total extra flight distance (c) Total delay

Figure 10: Performance metric for impacted flights within debris impact duration across different launch slots.

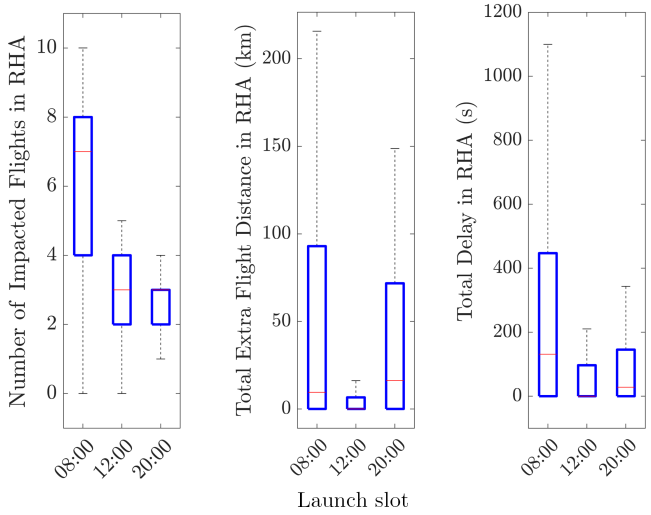

(a) Number of impacted flights (b) Total extra flight distance (c) Total delay

Figure 11: Performance metrics for flights during time delay related to ATM/STM coordination across different launch slots.

slot is scheduled for 20:00. This result is not surprising as the traffic is less during night time. The results suggest that, based on currently available data in Singapore FIR, it is possible to reduce the number of affected flights by more than 40% when performing the launch at night time (8 PM) compared to the morning (8 AM). This conclusion is preliminary and can be further verified with a large amount of flight data. However, Figure 11 (b) and (c) indicate that the variation in total extra flight distance and delay does not appear significant across different launch slots. A possible reason could be that although there are more flights in the morning and at noon, they do not enter the debris hazard area, and thus the trajectory after rerouting is not much different from the scheduled trajectory. This result also suggests that even if the evening is an ideal launch time, it's still crucial to optimize air traffic to minimize the impact of space launch hazards.

Next, we further assess the impact on aircraft due to time delays related to ATM/STM coordination. Figure 11 depicts the performance during the ATM/STM coordination if a space launch failure occurs. In this figure, we consider flights whose scheduled paths pass through the debris hazard area during this period. These findings are consistent with the results in Table II, indicating that a significant number of aircraft are still affected during this time. Also, the total extra flight distance and total delay is noteworthy considering the time delay, proving the necessity of the agent-based time delay modeling for improving the accuracy of air traffic analysis.

6. Conclusion

In this paper, the overview of space launch is firstly presented. A general ABM of space launch is then proposed in terms of the execution phase. To model the space launch failure and the associated impact to air traffic, we develop an ABM model to gain a comprehensive understanding of the complex interactions among entities involved in the execution phase. Several analysis metrics are defined to assess the impact of space launch hazard to air traffic operations. In the experiment, a Monte-Carlo simulation is designed to model on-trajectory space vehicle failure. A potential sea-based space launch in Singapore FIR is selected as a case study with initial analysis on flight delays and extra distance flown.

In future research, we will consider a variety of launch types, payload configurations, and launch parameters in simulation. Moreover, we plan to optimize more comprehensive space-launch presets, including launch window and dimension of hazard area, in addition to the launch locations discussed in this paper. In order to better align with real-world conditions, additional factors such as adverse weather conditions and wind effects will be taken into account. Lastly, calculating risk probabilities will be a key focus to enhance risk assessment.

7. Acknowledgement

This research is supported by the Office of Space, Technology and Industry (OSTIn) / Economic Development Board (EDB) of Singapore through the National Research Foundation (NRF) of Singapore Grant under the Space Technology Development Programme Grant. Gratitude is extended to RSAF CMDR (Retd.) Luke Neubronner, ATMRI, and CAAS colleagues for their feedback and comments that helped fine-tune the manuscripts. Any opinions, findings, and conclusions or recommendations expressed in this material are those of the author(s) and do not reflect the views of the OSTiN, EDB, NRF Singapore, or the Civil Aviation Authority of Singapore.

References

[1] W. Zhou, Q. Cai, and S. Alam, "A multi-task learning approach for facilitating dynamic airspace sectorization," in *Proceedings of International Workshop on ATM/CNS 2022 International Workshop on ATM/CNS*. Electronic Navigation Research Institute, 2022, pp. 192–199.

[2] Bryce tech, "Orbital and suborbital launch sites of the world 2023," 2023, https://brycetech.com/reports/report-documents/Bryce_Launch_Sites_2023.pdf. Accessed: 2023-11-01.

[3] E. Mathieu and M. Roser, "Space exploration and satellites," *Our World in Data*, 2022, https://ourworldindata.org/space-exploration-satellites. Accessed: 2023-11-01.

[4] R. Stilwell, "Flying high: Comparing the concepts for higher airspace operations in the us and europe," in *AIAA AVIATION 2023 Forum*, 2023, p. 3958.

[5] "Echo - european concept of operations for higher airspace operations," https://www.sesarju.eu/projects/echo, accessed: 2023-11-01.

[6] S. Kaltenhäuser, F. Morlang, T. Luchkova, J. Hampe, and M. Sippel, "Facilitating sustainable commercial space transportation through an efficient integration into air traffic management," *New Space*, vol. 5, no. 4, pp. 244–256, 2017.

[7] W. N. Chan, B. E. Barmore, J. L. Kibler, P. U. Lee, C. J. O'Connor, K. Palopo, D. P. Thipphavong, and S. J. Zelinski, "Overview of nasa's air traffic management-exploration (atm-x) project," in *AIAA Aviation Forum 2018*, no. ARC-E-DAA-TN57276, 2018.

[8] D. Murray, "The faa's current approach to integrating commercial space operations into the national airspace system," *Federal Aviation Administration*, 2013.

[9] J. L. Rouvroye and E. G. van den Bliek, "Comparing safety analysis techniques," *Reliability Engineering & System Safety*, vol. 75, no. 3, pp. 289–294, 2002.

[10] X. Pan, S. Ding, W. Zhang, T. Liu, L. Wang, and L. Wang, "Probabilistic risk assessment in space launches using bayesian network with fuzzy method," *Aerospace*, vol. 9, no. 6, p. 311, 2022.

[11] I.-s. Yoo, Y.-k. Seo, J.-h. Lee, B.-c. Song, and G.-r. Cho, "Risk management in korea space launch vehicle-i program," in *2006 IEEE International Conference on Management of Innovation and Technology*, vol. 2. IEEE, 2006, pp. 713–717.

[12] S. N. Sala-Diakanda, L. C. Rabelo, and J. A. Sepúlveda, "Case for a multidisciplinary modeling platform for space launch risk analysis," *SAE Transactions*, pp. 946–949, 2007.

[13] Y. D. Le, F. J. Wei, and A. Y. Liu, "The risk measurement of the space launch test project based on gray relational analysis," in *Advanced Materials Research*, vol. 718. Trans Tech Publ, 2013, pp. 686–691.

[14] D. L. Mathias, S. Go, K. Gee, and S. Lawrence, "Simulation assisted risk assessment applied to launch vehicle conceptual design," in *2008 Annual Reliability and Maintainability Symposium*. IEEE, 2008, pp. 74–79.

[15] S. Wilson, I. Vuletich, I. Bryce, M. Brett, W. Williams, D. Fletcher, M. Jokic, and N. Cooper, "Space launch & re-entry risk hazard analysis–a new capability," in *60th International Astronautical Congress (IAC), Daejeon, Korea*, 2009.

[16] O. J. Bojorquez and J. Chen, "Risk level analysis for hazard area during commercial space launch," in *2019 IEEE/AIAA 38th Digital Avionics Systems Conference (DASC)*. IEEE, 2019, pp. 1–6.

[17] L. L. Philipson, "Risk profile derivations for space and missile launch hazards," *Reliability Engineering & System Safety*, vol. 49, no. 3, pp. 217–236, 1995.

[18] G. Acciarini, F. Pinto, S. Metz, S. Boufelja, S. Kaczmarek, K. Merz, J. A. Martinez-Heras, F. Letizia, C. Bridges, and A. G. Baydin, "Spacecraft collision risk assessment with probabilistic programming," in *Third Workshop on Machine Learning and the Physical sciencedirects (NeurIPS 2020)*, 2020, pp. 1–6.

[19] E. Pate-Cornell and R. Dillon, "Probabilistic risk analysis for the nasa space shuttle: a brief history and current work," *Reliability Engineering & System Safety*, vol. 74, no. 3, pp. 345–352, 2001.

[20] T. J. Colvin and J. J. Alonso, "Compact envelopes and su-farm for integrated air-and-space traffic management," in *53rd AIAA Aerospace Sciences Meeting*, 2015, p. 1822.

[21] K. H. Van Dam, I. Nikolic, and Z. Lukszo, *Agent-based modelling of socio-technical systems*. Springer Science & Business Media, 2012, vol. 9.

[22] C. N. Bolczak, D. E. Boone, B. Lash, and C. E. Morgan, "Space launch and reentry operations collaborative decision making (cdm) concept," 2019.

[23] R. Frodge and D. Murray, "Space data integration," *Journal of Space Safety Engineering*, vol. 9, no. 2, pp. 182–188, 2022.

[24] Federal government of the United States, "The code of federal regulations - title 14 aeronautics and space," 2023, https://www.ecfr.gov/current/title-14.

[25] B. Bjelde, P. Capozzoli, and G. Shotwell, "The spacex falcon 1 launch vehicle flight 3 results, future developments, and falcon 9 evolution," *Space Exploration Technologies*, 2008.

[26] N. Brügge, "Evolution of the spacex merlin-1 engine," http://www.b14643.de/Spacerockets_2/United_States_1/Falcon-9/Merlin/index.htm.

[27] NASA Glenn Research Center, "Earth atmosphere model," 2021, https://www.grc.nasa.gov/www/k-12/airplane/atmosmet.html.

[28] R. Frodge and D. Murray, "Space data integration," *Journal of Space Safety Engineering*, vol. 9, no. 2, pp. 182–188, 2022.

[29] M. Rosenblatt, "Remarks on some nonparametric estimates of a density function," *The annals of mathematical statistics*, pp. 832–837, 1956.

[30] A. W. Bowman and A. Azzalini, *Applied smoothing techniques for data analysis: the kernel approach with S-Plus illustrations*. OUP Oxford, 1997, vol. 18.

[31] N. Dolan, J. Chen, J. C. Jones, and T. Reynolds, "Learning-based parameter optimization to support dynamic aircraft hazard area generation for space operations," in *AIAA Scitech 2021 Forum*, 2021, p. 0399.